REPORT DOCUMENTATION PAGE

Public reporting burden for this collection of information is estimated to average 1 hour per response, including the time for reviewing instructions, searching existing data sources, gathering and maintaining the data needed, and completing and reviewing the collection of information. Send comments regarding this burden estimate or any other aspect of this collection of information, including suggestions for reducing this burden to Washington Headquarters Services, Directorate for Information Operations and Reports, 1215 Jefferson Davis Highway, Suite 1204, Arlington, VA 22202-4302, and to the Office of Management and Budget, Paperwork Reduction Project (0704-0188), Washington, DC 20503

1. AGENCY USE ONLY (Leave Blank)	2. REPORT DATE 3/30/97	3. REPORT TYPE AND DATES COVERED 4/1/96-3/30/97

4. TITLE AND SUBTITLE

A Technique for Achieving 4000 Microstrain from Hard PZT

5. FUNDING NUMBERS

Grant# N00014-96-1-0711

6. AUTHOR(S)

Christopher S. Lynch

7. PERFORMING ORGANIZATION NAME(S) AND ADDRESS(ES)

Christopher S. Lynch
School of Mechanical Engineering
Georgia Institute of Technology
Atlanta, GA 30332-0405

8. PERFORMING ORGANIZATION REPORT NUMBER

9. SPONSORING/MONITORING AGENCY NAME(S) AND ADDRESS(ES)

Roshdy Barsoum
ONR 334, Office of Naval Research
Ballston Center Tower One
800 North Quincy Street
Arlington, VA 22217-5660

10. SPONSORING/MONITORING AGENCY REPORT NUMBER

19970327 069

11. SUPPLEMENTARY NOTES COR:

12a. DISTRIBUTION/AVAILABILITY STATEMENT

12b. DISTRIBUTION CODE

13. ABSTRACT (Maximum 200 words)

The year 1 effort was split between laboratory development and research. A smart materials laboratory was developed for research on the mechanics of electro-mechanical coupled materials. The laboratory includes sample preparation, test facilities, and failure analysis tools as described below. There are presently four graduate students working on this research, one at the masters level and three at the Ph.D. level. There have been two conference proceedings articles and one journal article submitted. This will substantially increase in the coming year. The PI has made four presentations of research results and will make an invited presentation in July, 1997. The PI is presently working on several related programs described below. Departmental support from Georgia Tech is being used to perform work in excess of the original scope of this project.

14. SUBJECT TERMS

Piezoelectric, Ferroelectric, Reliability

15. NUMBER OF PAGES

5

16. PRICE CODE

17. SECURITY CLASSIFICATION OF REPORT	18. SECURITY CLASSIFICATION OF THIS PAGE	19. SECURITY CLASSIFICATION OF ABSTRACT	20. LIMITATION OF ABSTRACT
unclassified	unclassified	unclassified	

Annual Report to the
Office of Naval Research

Due 3/30/97

A Technique for Achieving 4000 Microstrain from Hard PZT

PI:

Christopher S. Lynch
The G.W.W. School of Mechanical Engineering
The Georgia Institute of Technology
801 Ferst St. MRDC
Atlanta, GA 30332-0405

Annual Report to the

Office of Naval Research

Due 3/30/97

A Technique for Achieving 4000 Microstrain
from Hard PZT

Summary

The year 1 effort was split between laboratory development and
research. A smart materials laboratory was developed for research on
the mechanics of electro-mechanical coupled materials. The laboratory
includes sample preparation, test facilities, and failure analysis tools
as described below. There are presently four graduate students working
on this research, one at the masters level and three at the Ph.D. level.
There have been two conference proceedings articles and one journal
article submitted. This will substantially increase in the coming year.
The PI has made four presentations of research results and will make
an invited presentation in July, 1997. The PI is presently working on
several related programs described below. Departmental support from
Georgia Tech is being used to perform work in excess of the original
scope of this project.

Laboratory Development

Laboratory development occupied a substantial part of the contract
period. Table 1 lists the smart materials laboratory equipment acquired
from various sources (including this contract, $70k, test frame).

Table 1. Smart Materials Laboratory Equipment

Description	Cost
optical microscope w/DIC	$30k
scanning electron microscope	$30k
sample prep lab	$40k
test frame and associated equip.	$120k
Micro Moiré	$40k

The smart materials laboratory comprises equipment for sample preparation, testing, and failure analysis. The sample preparation equipment includes a diamond saw, grinding and polishing, an optical microscope, a vapor hood, and cabinetry/counters. Test equipment includes a load frame (purchased under this contract), a 20 kV power supply, an in-situ video based microscope with transmitted and reflected polarized light capability, fixtures for compression with electric field and compact tension with electric field, strain gauge amplifiers, and a computer based controller with multiple channel control and phased function generators. The failure analysis equipment includes a JOEL 840 scanning electron microscope, and an optical microscope with DIC.

Student/Post Doctoral Support

Four graduate students are working in this research area. Some of the student support is being provided by Georgia Tech as new faculty support. Will Stoll will complete a masters thesis on the non-linear and hysteretic behavior of commercial PZT in June 1997. Wei Chen has completed a micromechanics based modeling effort for tetragonal and rhombohedral structures. He is using the results in the development of continuum mechanics based constitutive laws using an internal

state variable approach. This model shows promise for implementation in commercial finite element codes, providing a design tool for both actuator developers and active structures designers. Don Upton is working on the masters portion of a Ph.D. program. He is measuring the time and temperature dependent response of commercially available actuator materials. Haihui Niu is working on the development of a J-integral test technique that uses the load-displacement and the voltage-charge curves from compact tension specimens to determine the energy release rate. J. Fan will be joining the project soon as a post doctor working on the implementation of the phenomenological constitutive laws in FEM codes.

Publications/Presentations

Journal articles submitted:
    C.S. Lynch, "Fracture of ferroelectric and relaxor electro-ceramics: influence of electric field", submitted to Acta Materialia, 3/14/97

Book chapter written (partially related to this project)
    Lynch, C.S., *Strain Measurement Techniques*, The Measurements, Instrumentation, and Sensors Handbook, A CRC Press, Inc. Publication, J.G. Webster ed., 1997

Proceedings articles submitted
    Lynch, C.S. with W. Stoll, "Experimental Measurements of Electro-Mechanical Behavior of Four Compositions of PZT, Proceedings of the 1996 IEEE International Symposium on the Application of Ferroelectrics
    Lynch, C.S. "J-Integral for Ferroelectric Compact Tension Specimens with Electric Field", SPIE 1997 Symposium on Smart Structures and Materials San Diego, Ca. Mar 1997

Presentations
    3/19/96 Constitutive behavior of ferroelectric ceramics, Cambridge University, Cambridge U.K. (Invitation by Norman Fleck)
    3/21/96 Constitutive behavior of ferroelectric ceramics, Leicester University, Leicester U.K. (Invitation by Alan Cocks)
    7/18/96 Constitutive Behavior and Design Interrelations for PZT Actuators, Northrop Aircraft, Hawthorn CA (Invitation by Dr. Jay Kudva)
    8/22/96 Poster Presentation, "Experimental Measurements of Electro-Mechanical Behavior of Four Compositions of PZT", Proceedings of the 1996 IEEE International Symposium on the Application of Ferroelectrics
    12/2/96 "Stress/Strain/Electric Field Measurements on Hard and Soft PZT", Materials Research Society, Boston MA, Dec. 1996
    7/97 Invited talk to be given at Banff, $500 honorarium, technology overview.

Two additional journal article manuscripts are near completion, one on the constitutive behavior of commercial compositions of PZT and a second on J-integral testing of electro-mechanically coupled ceramics.

Collaboration

The PI is involved in several related research projects outlined in Table 2.

Table 2. Related Research and Collaboration

Title	Funding Agency	Amount	Period
Smart Wing	ARPA/Northrop	$30,000	1/96 to 5/97
A Technique for Achieving 4000 microstrain from hard PZT	ONR Young Investigator	$370,000	4/96 - 3/99
Smart Wing Phase II*	DARPA/Northrop	$150,000	6/97-5/00
TRS/DARPA Actuator	DARPA/TRS	$105,000	6/97-5/99

*budget to be negotiated

In addition, the PI is negotiating a consulting arrangement with United Technologies, Pratt and Whitney to help with piezoelectric actuator characterization and qualification for aircraft applications.

University Support

Georgia Tech is continuing to provide support for graduate students and a light teaching load for the PI. The school of mechanical engineering is providing no cost machinist and shop time as well as no cost electrical engineer and electronics technician shop time.

Additional Information

Copies of articles are attached.

A Technique for Achieving 4000μStrain from Hard PZT — Office of Naval Research, Sponsor

Christopher S. Lynch
School of Mechanical Engineering
Georgia Institute of Technology
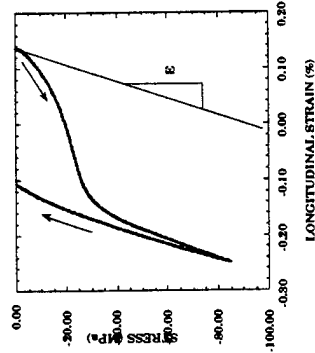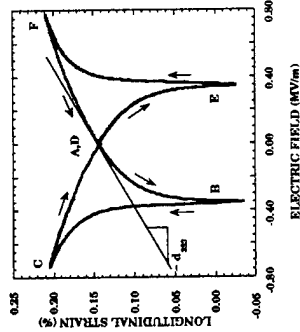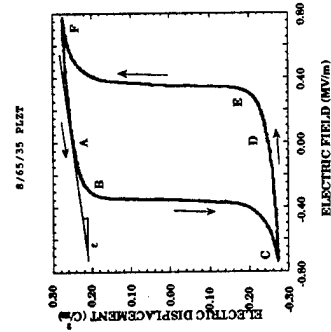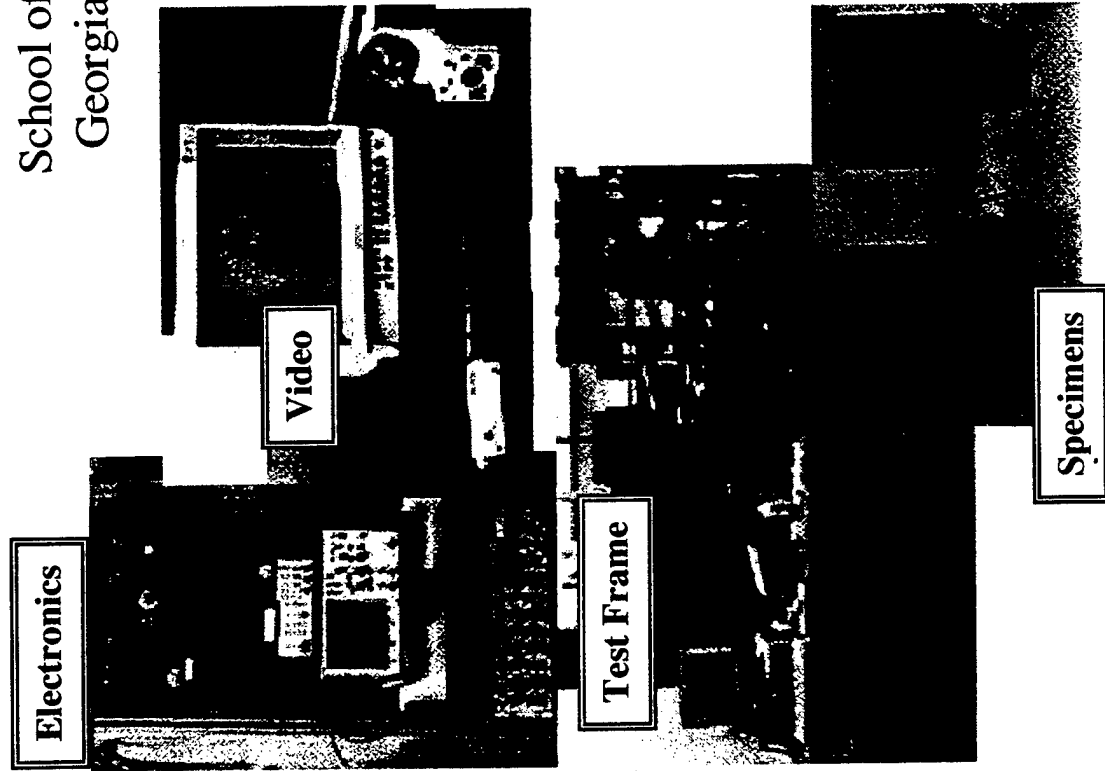
Approach:
Experimental Measurement of Polarization Switching Behavior

Impact:
Operation Across Switching Thresholds without Cracking. Much Larger Strain.

Preliminary Results:
1. Constitutive Measurements on Five Compositions of PZT, PLZT.
2. Toughness Measurements on Piezoelectric and Relaxor PLZT with E-Field.
3. Developed Internal State Variable Framework for Constitutive Models.
4. Extended Micromechanics Model to Rhombohedral and Orthorhombic Structures.

Electronics

Video

Test Frame

Specimens

Fracture of Ferroelectric and Relaxor Electro-Ceramics: Influence of Electric Field

Christopher S. Lynch

The G.W. Woodruff School of

Mechanical Engineering

The Georgia Institute of Technology

Atlanta, Georgia 30332-0405

Fracture of Ferroelectric and Relaxor Electro-Ceramics: Influence of Electric Field*

Christopher S. Lynch

The G.W. Woodruff School of

Mechanical Engineering

The Georgia Institute of Technology

Atlanta, Georgia 30332-0405

ABSTRACT

Crack growth is studied in a ferroelectric and a relaxor composition of lead lanthanum zirconate titanate (PLZT) ceramic using Vicker's indentations with electric field. The polarized ferroelectric composition displays excess crack growth perpendicular to the polarization direction. This excess crack growth is increased by an electric field in the polarization direction. The relaxor composition does not display this excess crack growth. Results suggest that the excess crack growth perpendicular to the polarization is the result of intergranular residual stress.

I. INTRODUCTION

The Vicker's indentation test technique[1,2,3] involves pressing a square diamond pyramid into a sample with a known force. The resulting wedge force drives radial cracks. Polarized ferroelectric ceramics display increased radial crack growth[4-8] perpendicular to the polarization. A DC electric-field in the direction of the polarization enhances this effect[7,9]. The opposite effect has been observed in relaxor compositions. In quadratic electrostrictors, electric field hinders crack growth perpendicular to the applied field[10].

Several microstructural variables interact with crack growth in ceramics. Intergranular residual stress that arises from anisotropic strain of the crystal structure can result in microcracking, usually along grain boundaries[11]. Rice and Freiman[12,13] demonstrated that the fracture energy of a number of ceramics with anisotropic thermal expansion increases with grain size, reaches a peak, then falls with an additional increase in grain size. Pohanka, Freiman, and Rice[14] include these effects in their expression for the energy release rate of ferroelectric ceramics.

In ferroelectric ceramics, residual stress is associated with the phase transformation (from cubic to tetragonal, orthorhombic or rhombohedral) that occurs on cooling through the Curie temperature. In the absence of twinning (non-180° domain formation) the magnitude is independent of grain size and proportional to the transformation strain and the elastic modulus. At large grain sizes this residual stress is observed to induce spontaneous cracking[15]. At the Curie point, barium titanate (BT) spontaneously microcracks at a grain size of 100μm and lead titanate (PT) spontaneously microcracks and reduces to powder at a grain size of 1-10μm.

Dopants are used to harden or soften lead zirconate titanate (PZT)[16]. This affects both the mechanical and electrical properties by hindering or enhancing

twinning. Hard PZT shows less hysteresis and a greater resistance to polarization switching under stress or electric field loading[17,18] than does soft PZT.

Electric field is postulated to interact with the fracture toughness of ferroelectric ceramics altering the intergranular residual stress through removing twins and piezoelectrically or electrostrictively distorting the grains. This results in intergranular incompatible strains and stresses. Electric field also directly interacts with cracks due to the difference in the dielectric permittivity of the ceramic and the cracks' interiors[19-22]. This permittivity difference results in electric field concentrations.

Relaxor compositions in the quadratic electrostrictive state have little or no residual stress. Domains spontaneously nucleate and grow on the 100 nanometer size scale. Application of electric field preferentially grows domains in the direction of the applied field, but not sufficiently to induce a large component of residual stress.

II. EXPERIMENTS

The purpose of the experiments is to determine the necessary conditions for extended crack growth and find whether this extended crack growth can be explained by residual stress and electric field interactions. The material selected for these tests was PLZT, a relaxor ferroelectric[23,24]. Two compositions were selected, 8/65/35 and 9.4/65/35 (at%La/PZ/PT). At room temperature 8/65/35 is below the lower transition temperature and is ferroelectric, while 9.4/65/35 is at its dielectric maximum in the transition zone and is quadratic electrostrictive. The properties are listed in Table 1. Both have a rhombohedral crystal structure and an average 5 μm grain size.

A Vicker's indentation system was modified to accommodate application of electric field during the indentation process. Indentations were performed with and without electric field and at several temperatures on unpoled and poled ferroelectric samples and on quadratic electrostrictive samples. Tests were performed in immersion oil.

Indentations on unpoled samples of both compositions at several mechanical loads (with E=0) formed a reference data set. (Unpoled samples have no electro-mechanical coupling and have isotropic properties.) The indented samples were then subjected to electric field to determine the interaction between electric field, radial cracks, and the residual stress field left by the indentation process. Next, indentations were performed in the presence of a DC electric field to measure the effect of the interaction between the electric field, the stress field, and the radial cracks during crack growth. Finally, indentations were performed on a polarized ferroelectric specimen (piezoelectric in this state) at various electric field levels (applied in the direction of the polarization) ranging from zero to greater than the coercive field to assess the interaction of polarization, electric field, and the radial crack system.

III. RESULTS

Vicker's indentations in the unpoled ceramic resulted in symmetric radial crack growth (Fig. 1a). When the ferroelectric composition was polarized prior to indentation, increased crack growth perpendicular to the polarization direction was observed (Fig. 1b). When indentations were performed in the ferroelectric composition at twice the coercive field level, there was substantially more crack growth perpendicular to the field direction, and distributed damage in the vicinity of the indentation (Fig. 1c). In the unpoled state the indent diagonal and the radial crack lengths were labeled 2a and 2c (Fig. 1d). In the poled state, or in the presence

of electric field, the radial cracks were labeled with the angle relative to the polarization direction; 2c 0°, and 2c 90° (Fig. 1e).

A. Radial crack growth in non-polarized specimens

In the unpoled state the 8/65/35 specimen is ferroelastic and both the 8/65/35 and the 9.4/65/35 specimens have isotropic elastic properties. Indentations were performed using several indentation loads. Radial crack size increased with indentation load (Fig 2). The 8/65/35 and 9.4/65/35 displayed similar amounts of crack growth at low loads (short cracks) and the 8/65/35 displayed less crack growth than the 9.4/65/35 at higher loads (longer cracks). The indentation size, 2a, was the same for both compositions and increased with load.

B. Electric field applied to existing indentations

An 8/65/35 specimen was prepared with electrodes and lead wires. Indentations were performed in the face mid way between the electrodes at two different mechanical loads. The specimen was then subjected to a ramp in electric field. The field was increased to a fixed level then decreased to zero and the radial crack length measured. This electric field cycle was performed several times at increasing field levels and the radial crack length remeasured after each cycle (Fig. 3). When the electric field amplitude reached 0.3 MV/m, the radial cracks extended. This field level is approximately 75% of the coercive field. The cracks perpendicular to the field extended approximately 30%.

Similar tests were performed on the quadratic electrostrictive 9.4/65/35 composition (Fig. 4). The electric field induced a very small amount of crack extension.

C. Indentations performed in the presence of electric field

Indentations were performed in the ferroelectric 8/65/35 composition (initially in the unpoled state) with electric field present. A DC electric field was applied, the indentation performed, the indenter removed, the field reduced to zero, and the crack lengths measured (Fig. 5). Indentations were performed at various loads and electric field levels. Electric field had little or no effect until it was near the coercive field, at which point it induced additional crack growth. The maximum applied field of 0.3 Mv/m was below the coercive field. The additional crack growth induced by the electric field appears to be a function of the electric field and independent of indent load rather than a fixed percentage of the zero field crack length associated with that load.

Similar tests were performed on the quadratic electrostrictive 9.4/65/35 composition (Fig. 6). There was a slight decrease in crack growth in the presence of electric field.

D. Indentations performed in a pre-polarized ferroelectric composition with electric field present

Indentations were performed with a 4 kg load on the ferroelectric 8/65/35 specimens at several electric field levels. The specimens were first polarized by the application of several electric field cycles at twice the coercive field. Anisotropic crack growth was observed at zero electric field (Fig. 7). As the electric field was increased, the indentations produced radial cracks that were shorter parallel to the electric field direction and longer perpendicular to the field direction. This effect seemed to saturate at 0.5 Mv/m, about 1.2 times the coercive field.

When indented under high electric field, the ferroelectric composition developed a series of microcracks in the stress field of the indentation (Fig. 1.c). These were not extensions of the radial or lateral crack systems.

E. Indentations performed at various temperatures

Indentations were performed in unpoled specimens at various temperatures. The morphology of the cracks changed as the temperature was increased, with more microcracking around the indentation zone and less well developed radial cracks. In some of the indents, the radial cracks branched at odd angles relative to the indent axes. Only the data from symmetric radial cracks were plotted (Fig. 8). The indentation diagonals, 2a, were nearly independent of temperature. The crack length of the 8/65/35 composition increased as the temperature was increased to 100°C. At 100°C, the 8/65/35 composition has quadratic electrostrictive behavior, the same as the 9.4/65/35 composition at room temperature. The crack lengths in the 9.4/65/35 composition increased with temperature. At 100°C this composition is nearly cubic.

F. Other Tests

A series of tests were performed without the immersion oil. Radial crack lengths were comparable to those performed through a drop of oil. The samples indented in air were placed in a container of distilled water for 24 hours and then the radial crack lengths were remeasured. No additional crack growth was observed.

IV. DISCUSSION

Several variables affect crack growth in ferroelectric ceramics. The data from this study help to identify those that cause extended crack growth in polarized ferroelectric ceramics. The experimental results indicate that, at the field levels tested, extended crack growth is associated with approaching the coercive field in the ferroelectric composition. An additional observation of Mehta and Virkar[4] is

7

important to the following discussion. In their study, lead zirconate titanate was mechanically poled by application of compressive stress (ferroelastic switching). Specimens poled in this way were not piezoelectric, yet displayed the extended crack growth. This suggests piezoelectric coupling to the crack tip stress field is not a critical mechanism for extended crack growth.

The test results are discussed in terms of the energy release rate. This is the energy dissipated per unit advance of the crack per unit crack width. The energy release rate G, is written as the sum of contributions from several dissipative mechanisms that are active in the high stress, high electric field zone found at the tip of the crack, equation (1).

$$G = 2\gamma_s + \gamma_{\mu c} + \gamma_t + \gamma_r + \gamma_{pt} \qquad\qquad 1.$$

where $2\gamma_s$ is the surface energy needed to create the two crack surfaces, $\gamma_{\mu c}$ is the energy absorbed by microcrack formation, γ_t is the energy expended in ferroelastic twinning the crystal structure, γ_r is the energy the residual stress contributes to driving the main crack (a negative term), and γ_{pt} is the energy contributed by a dilational phase transformation. The crystal structure of the compositions used in this study is rhombohedral. Little or no stress induced phase transformation is expected, thus the last term is considered negligible.

Residual stress, microcracking, and twinning are coupled with electric field in ferroelectric ceramics. Residual stress arises from the anisotropic deformation of individual grains in the ceramic that is associated with the phase transformation as the ceramic is cooled through the Curie point. This anisotropic deformation is relieved by ferroelastic twining. In relaxors, a very fine domain structure forms as the material is cooled, leaving nearly zero residual stress in the as cooled state. Application of electric field in excess of the coercive field removes most or all of the

8

twins, resulting in single domain grains. In this state, the intergranular residual stress is large. When the intergranular residual stress is high enough and nucleation sites for grain boundary fracture are available, microcracking occurs along the tensile portion of the grain boundaries.

Residual stress, microcracking, and twinning influence crack propagation. Residual stress interacts with the fracture process in the following way: When a crack propagates through the ceramic, the stored strain energy density associated with residual stress is relieved on the crack face on the order of one grain diameter in depth. The strain energy released is proportional to the grain size. At small grain sizes there is little residual strain energy released as a crack propagates. At intermediate grain sizes the residual stress helps to propagate the main crack, and microcracks can form in the tensile crack tip field at grain boundaries that were under residual tension. If the residual strain energy released by a grain is not sufficient to source the surface energy required to form a microcrack, then the microcrack absorbs energy and the energy release rate is increased. At larger grain sizes, the residual strain energy released is sufficient to source the surface energy for the microcrack. In this case the contribution to the energy release rate is negative and the toughness is decreased. Microcrack formation is localized to a crack tip process zone when intrinsic flaws are small enough that the crack tip stress concentration is required to nucleate grain boundary flaws into microcracks. At even larger grain sizes, there is sufficient residual strain energy available to spontaneously microcrack the ceramic.

A relationship between residual stress and the contribution of microcracking to the energy release rate is developed by considering a main crack surrounded by a small scale microcrack cloud. Let $B\Delta a$ be the area increase of the main crack per crack advance Δa, where B is the width of the crack, and let $nB\Delta a$ be the area

increase of microcracks per crack advance Δa where n is the ratio of microcrack area formed to new crack surface formed.

The irreversible work done to advance the crack is equal to the work done to form the new crack surface less the residual stress contribution to the propagation of the main crack, plus the work done in creating microcrack surface in the crack tip process zone less the work done by releasing residual strain energy at each microcrack plus the work done in driving ferroelastic twinning. This energy balance is written as Equation (2).

$$W = 2\gamma_s B\Delta a - 2B\Delta a d\,\sigma_R^2/2E + 2\gamma_s nB\Delta a - 2nB\Delta a d\,\sigma_R^2/2E + \gamma_t B\Delta a \qquad 2.$$

where γ_s is the surface energy, B is the specimen thickness, n is the area increase of microcracks created per unit area increase of the main crack, d is the average grain diameter, σ_R is the magnitude of the tensile component of residual stress, E is the Young's modulus, and γ_t is the energy absorbed per unit crack advance per unit width by ferroelastic twinning. Dividing by BΔa gives an expression for the energy release rate in the presence of residual stress and twinning, equation (3).

$$G = (1+n)(2\gamma_s - d\sigma_R^2/E) + \gamma_t \qquad 3.$$

In equation (3), n is a function of σ_R, the size and distribution of grain boundary flaws, and the grain size. This function must be known to calculate G. The behavior of equation (3) describes observed material behavior. At small d, n tends toward zero (no microcracking) and the surface energy term is much larger than the intergranular stress term. As the grain size d, increases, n increases. This corresponds to the formation of microcracks near the primary crack tip. This increases G. As d further increases, the intergranular residual stress contribution

to fracture becomes larger. This term is negative and thus G begins to decrease. Further increase of grain size eventually leads to a negative energy release rate. This corresponds to spontaneous microcracking. Equation (3) captures the observed behavior of ceramics with anisotropic thermal expansion of the crystal structure. In these materials the energy release rate increases with grain size then decreases and goes to zero at a large grain size[12-15]. At sufficiently large d, there is enough residual strain energy available to spontaneous microcrack the ceramic. Laws could be developed relating the height of a microcrack zone to the residual stress and grain size, possibly taking the intrinsic flaw size proportional to d.

A sample calculation using equation (3) shows that the results are reasonable. The surface energy is determined from the fracture toughness of the unpoled material (K_{Ic} = 0.75 MPa$\sqrt{m}$) and the Irwin relation (G=(1-v^2)/E K_{Ic}^2) as γ_s = 6.2 J/m^2. The residual stress in the presence of a high electric field is estimated from the single crystal saturation strain ($\varepsilon^s \approx 3.5x10^{-3}$) and the Young's modulus (E=68 GPa). Taking n=0 (no microcrack cloud), γ_t=0 (no twin toughening at high electric field), and d=5x10^{-6} m, equation (3) predicts the energy release rate will be reduced from 12.4 to 8 J/m^2 by application of a strong electric field. Clearly a more rigorous analysis is needed to calculate the contribution of intergranular residual stress to the reduction in energy release rate. This order of magnitude calculation however, strongly supports the postulate that intergranular residual stress induced by remanent strain is the cause of the observed excess crack growth.

Intergranular residual stress is a function of electric field. When polarized, the residual stress is largest in the direction of polarization. Some of this residual stress is relieved by ferroelastic twinning (aging). Application of electric field in the direction of the polarizing field increases the intergranular residual stress and removes twins. At the grain sizes tested, the increase of intergranular residual stress with electric field reduces the energy release rate. The removal of twins also

11

removes the twin toughening component. An electric field in the opposite direction reduces residual stress and increases the amount of twinning available for toughening the ceramic.

When indentations were performed in the ferroelectric composition in the presence of a strong electric field, cracking occurred in the tensile stress field of the indenter but independent of the main crack (Fig 1.c). This is a spreading of the microcracking away from the crack tip zone. At high electric field this material is very near the threshold of spontaneous microcracking.

Other mechanisms interact with crack growth in electro-mechanically coupled ceramics. There is some twin toughening associated with the cracks that run parallel to the polarization. This slightly decreases crack growth in this direction in poled specimens. There is also a negative contribution to the energy release rate[19] caused by a jump in dielectric permittivity from the material to the crack interior. This accounts for the slight decrease in crack growth perpendicular to an applied electric field in the relaxor composition.

The reduction of toughness by intergranular residual stress also explains earlier observations of electric field driven fatigue crack growth by Cao and Evans[25] and by Lynch et al[26]. These cracks are observed to grow from Vicker's indentations perpendicular to the polarization in ferroelectric compositions driven by cyclic electric field above the coercive field. The cracks extend about 40 μm each half cycle, depending on electric field level. This type of fatigue crack growth does not occur in quadratic electrostrictors.

V. CONCLUDING REMARKS

The anisotropic crack growth observed when Vicker's indentations are performed in poled ferroelectric ceramics was discussed in terms of an intergranular

contribution to the energy release rate. The effect of residual stress is much larger than other mechanisms that interact with crack propagation. The results were not presented in terms of calculated toughness since the Vicker's indentation technique has not been calibrated for anisotropic materials. There is, however, a drop in fracture toughness perpendicular to the polarization direction that needs to be quantified for these materials. An equation was developed that describes the residual stress contribution to toughness by balancing the work of fracture with the energy absorbed in forming new surfaces less the residual strain energy released. The results indicate that smaller grain size ferroelectric ceramics will have a higher toughness perpendicular to the polarization, and that smaller grain size may reduce or eliminate the spontaneous cracking that can occur during polarization switching. It is also clear from the model that microcracking can be avoided by operating at field levels below the saturation level, and that it may be possible to increase the reliability of ferroelectric ceramic actuators by not fully polarizing the ceramic. If some twins are left in the crystal structure, they will relieve some of the intergranular residual stress.

VI. ACKNOWLEDGMENTS

VII. REFERENCES

1. Anstis G.R., Chantikul, P., Lawn, B.R., Marshall, D.B., "A Critical Evaluation of Indentation Techniques for Measuring Fracture Toughness: I, Direct Measurements" *J. Am. Ceram. Soc*, **64** (9), 533-538, 1981

2. Braun L.M., S.J. Bennison, B.R. Lawn, "Objective Evaluation of Short Crack Toughness Curves Using Indentation Flaws: Case Study on Alumina-Based Ceramics", *J. Am. Ceram. Soc.*, 75[11] 3049-57 (1992)

3. Marshall D.B., B.R. Lawn, "An Indentation Technique for Measuring Stresses in Tempered Glass Surfaces", *J. Am. Ceram. Soc.* 60 [1,2] Jan-Feb (1977)

4. Mehta K., A.V. Virkar, "Fracture Mechanisms in Ferroelectric-Ferroelastic Lead Zirconate Titanate (Zr:Ti=0.54:0.46) Ceramics", J. Am. Ceram. Soc. 73[3] 567-74 (1990)

5. Esaklul K.A., W.W Gerberich, B.G. Koepke, "Stress relaxation in PZT", J. Am. Ceram. Soc. 63[1,2], 25-30, (1980)

6 Pisarenko, G.G., V.M. Chushko, and S.P. Kovalev, "Anisotropy of Fracture Toughness of Piezoelectric Ceramics", *J. Am. Ceram. Soc.*, **68** [5] 259-65, 1985

7. Tobin A.G., Y.E. Pak, "Effect of electric field on fracture behavior of PZT ceramics", Proceedings SPIE Vol. 1916/79, March (1993)

8. Okazaki K., "Mechanical behavior of ferroelectric ceramics", Ceramic Bulletin, 63[9] (1984)

9. Sun C.T., S.B. Pak, "Determination of fracture toughness of piezoelectrics under the influence of electric field using Vicker's indentation", School of Aeronautics and Astronautics, Purdue University, unpublished work

10. Raynes A.S., G.S. White, S.W. Freiman, B.S. Rawal, "Electric field effects in a lead magnesium niobate ceramic", NIST (need reference)

11. Evans A.G., "Microfracture from Thermal Expansion Anisotropy-I. Single Phase Systems", *Acta. Met.* 26, 1845-53 (1978)

12. Rice R.W., S.W. Freiman, P.F.Becher, "Grain-Size Dependence of Fracture Energy in Ceramics: I, Experiment", *J. Am Ceram. Soc,* 64[6], 345, June (1981)

13. Rice R.W., S.W Freiman, "Grain -Size Dependence of Fracture Energy in Ceramics: II, A Model for Noncubic Materials" *J. Am Ceram. Soc,* 64[6], 350, June (1981)

14. Pohanka R.C., S.W. Freiman, R.W. Rice, "Fracture Processes in Ferroic Materials", Ferroelectrics, 28, 337-342, (1980)

15. Rice R.W., R.C. Pohanka, "Grain Size Dependence of Spontaneous Cracking in Ceramics", *J. Am Ceram. Soc*, 61[11-12], 559, Dec (1979)

16. Jaffe B., W.R. Cook, H. Jaffe, "Piezoelectric Ceramics", Academic Press, London and N.Y. (1971)

17. Cao H.C., A.G. Evans, "Nonlinear Deformation of Ferroelectric Ceramics", J. Am. Ceram. Soc., 76[4] 890-96, (1993)

18. Lynch C.S., "The effect of uniaxial stress on the electro-mechanical response of 8/65/35 PLZT", Submitted to Acta. Met. (1995)

19. Suo Z., "Mechanics Concepts for Failure in Ferroelectric Ceramics", in *AD-Vol. 24/AMD-Vol. 123, Smart Structures and Materials, ASME Proceedings*, 1991

20. McMeeking, R.M., "Electrostrictive Stress near Crack-like Flaws," *J. Appl. Math. Phys.* **40**, 615-627 (1989)

21. Yang, W. and Z. Suo, "Cracking in Ceramic Actuators Caused by Electrostriction", *J. Mech. Phys. Solids*, 42[4], 649-63, (1994)

22. Suo, Z., "Models for Breakdown-Resistant Dielectric and Ferroelectric Ceramics," *J. Mech. Phys. Solids.* **41**, 1155-1176, 1993.

23. Cross, L.E., "Relaxor Ferroelectrics", *Ferroelectrics,* **76**, 241-267, 1987

24. Haertling, G.H., 1987, "PLZT Electrooptic Materials and Applications-A Review," *Ferroelectrics*, **75**, 25-55.

25. Cao H.C., A.G. Evans, "Electric Field Induced Fatigue Crack Growth in Ferroelectric Ceramics", *J. Am. Ceram Soc* (in press 1995)

26. Lynch C.S., W. Yang, L. Collier, Z. Suo, R.M. McMeeking, "Electric Field Induced Cracking in Ferroelectric Ceramics", Accepted for Publication in Ferroelectrics, (1994)

LIST OF FIGURES

Figure 6. Indentations are performed in the presence of electric field on the 9.4/65/35 quadratic electrostrictive composition. The presence of electric field may slightly hinder crack growth, but the amount is not significant.

Figure 7. Indentations in the polarized 8/65/35 composition in the presence of electric field. As the electric field is increased, the cracks perpendicular to the polarization direction become longer. This effect saturates just above the coercive field.

Figure 8. Crack length and indentation size produced by a 3 kg load are measured at various temperatures. The indentation size is independent of temperature. Crack growth increases with temperature. The 8/65/35 composition goes from ferroelectric to quadratic electrostrictive behavior over this temperature range. The 9.4/65/35 composition goes from quadratic electrostrictor to cubic paraelectric behavior over this temperature range. As the availability of twinning decreases, crack growth increases.

TABLE I. PROPERTIES OF PLZT

Composition (%La/Zr/Ti)	8/65/325	9.5/65/35
d_{33} (x10^{-12} C/N)	682	0
P^R (C/m^2)	.30	0
Ec (MV/m)	3.6	0
Tc (°C)	110	25
25°C Phase	Ferro. Rh.	
ε_r	3350	5500
tan δ (%)	2.5	5.5
resistivity (Ω-cm)	10^{13}	10^{13}
k	.648	0
S_{11} (x10^{-12} m^2/N)	12.4	12.4
Q_{11} (m^4/C^2)	.018	.021
Q_{12} (m^4/C^2)	-.008	-.009

Figure 1. a. Photograph of a symmetric indentation characteristic of an unpoled ferroelectric (width of field 500μm). b. Photograph of an asymmetric indentation characteristic of a ferroelectric composition poled in the vertical direction (width of field 1 mm). c. Photograph of an indentation in the ferroelectric composition 8/65/35 indented under an electric field of 0.8 Mv/m (width of field 3 mm). Note the peripheral microcracking that occurred in the stress field of the indentation. Back lighting gives the cracks the dark appearance.
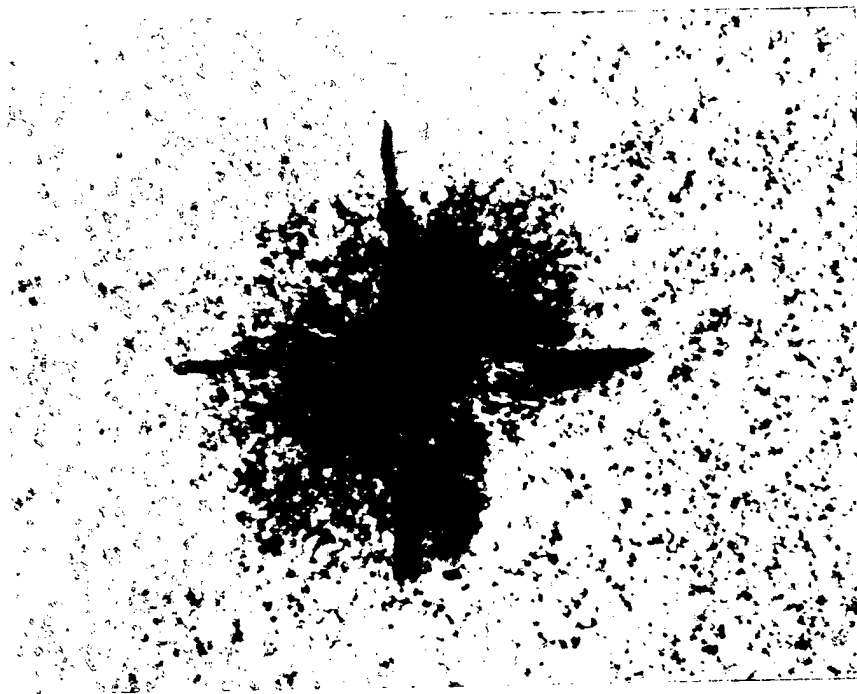
Figure 1. d. Crack labeling for symmetric indentations. e. Crack labeling for asymmetric indentations.

Figure 2. Crack length and indentation size vs. indent load for 9.4/65/35 and unpoled 8/65/35PLZT. At higher loads the cracks are shorter in the ferroelectric composition.

Figure 3. Two indentations are monitored as electric field is increased to just below the coercive field, one produced with 1.5 kg load and one with 6 kg load. When the electric field nears the coercive field, the cracks perpendicular to the electric field grow and the cracks parallel to the polarization do not.

Figure 4. Three indents in 9.4/65/35 PLZT are monitored as electric field is applied. The electric field induces a small amount of crack growth.

Figure 5. Indentations are performed in the presence of electric field in the 8/65/35 unpoled ferroelectric composition. Crack growth is not affected by electric field until the coercive field is approached.

Figure 6. Indentations are performed in the presence of electric field on the 9.4/65/35 quadratic electrostrictive composition. The presence of electric field may slightly hinder crack growth, but the amount is not significant.

Figure 7. Indentations in the polarized 8/65/35 composition in the presence of electric field. As the electric field is increased, the cracks perpendicular to the polarization direction become longer. This effect saturates just above the coercive field.

Figure 8. Crack length and indentation size produced by a 3 kg load are measured at various temperatures. The indentation size is independent of temperature. Crack growth increases with temperature. The 8/65/35 composition goes from ferroelectric to quadratic electrostrictive behavior over this temperature range. The 9.4/65/35 composition goes from quadratic electrostrictor to cubic paraelectric behavior over this temperature range. As the availability of twinning decreases, crack growth increases.

Figure 1.a

Figure 1.b

Figure 1.c

Figure 1. d. Crack labeling for symmetric indentations. e. Crack labeling for asymmetric indentations.

Figure 2. Crack length and indentation size vs. indent load for 9.4/65/35 and unpoled 8/65/35PLZT. At higher loads the cracks are shorter in the ferroelectric composition.
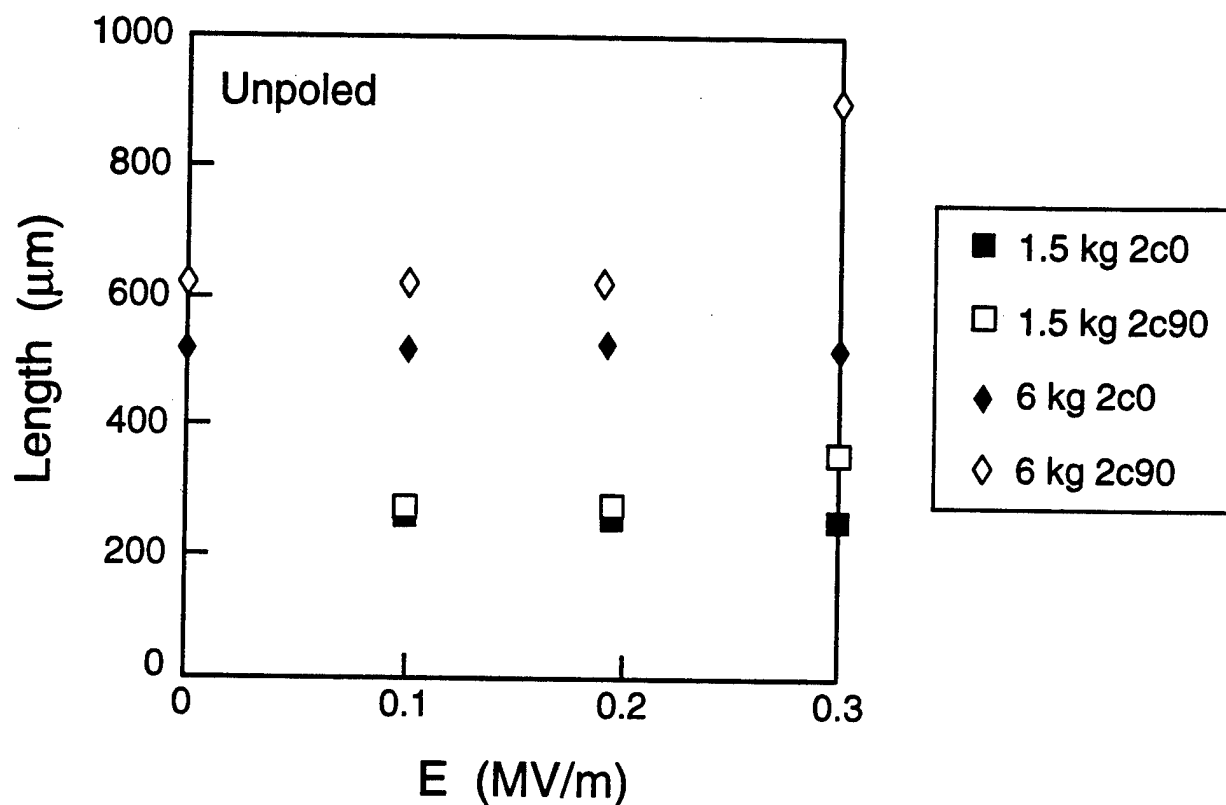
Figure 3. Two indentations are monitored as electric field is increased to just below the coercive field, one produced with 1.5 kg load and one with 6 kg load. When the electric field nears the coercive field, the cracks perpendicular to the electric field grow and the cracks parallel to the polarization do not.

Figure 4. Three indents in 9.4/65/35 PLZT are monitored as electric field is applied. The electric field induces a small amount of crack growth.
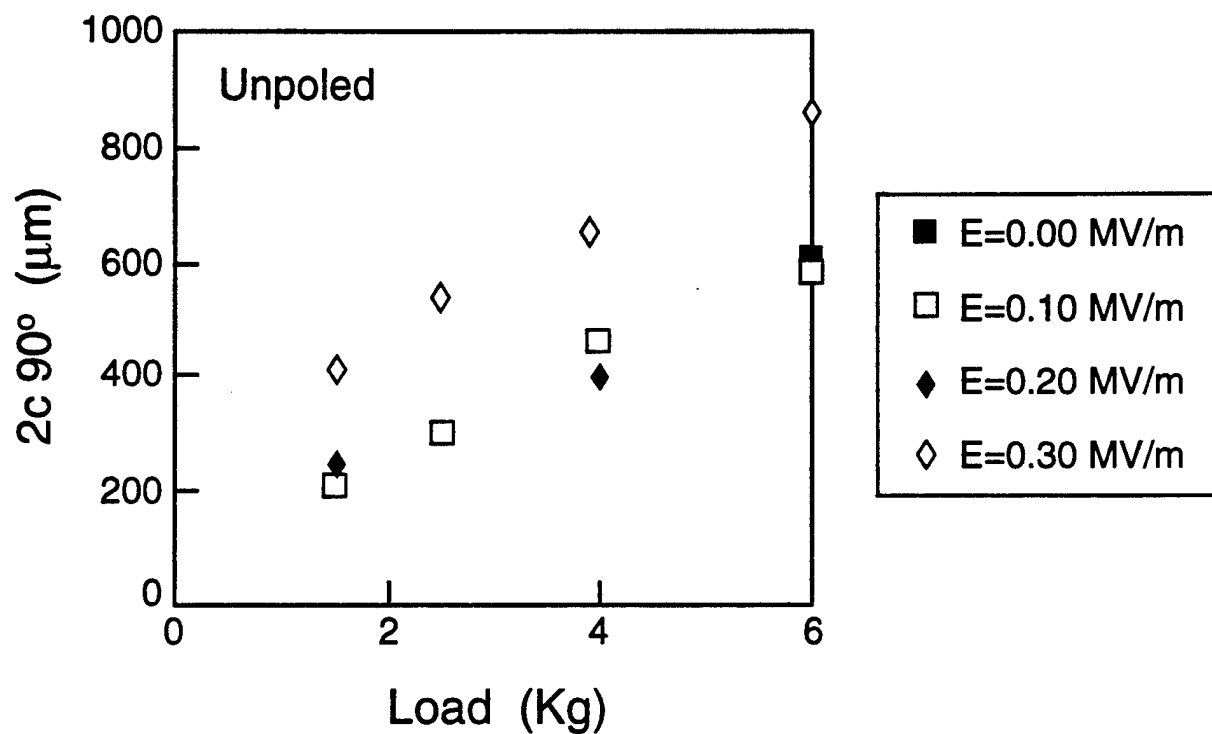
Figure 5. Indentations are performed in the presence of electric field in the 8/65/35 unpoled ferroelectric composition. Crack growth is not affected by electric field until the coercive field is approached.
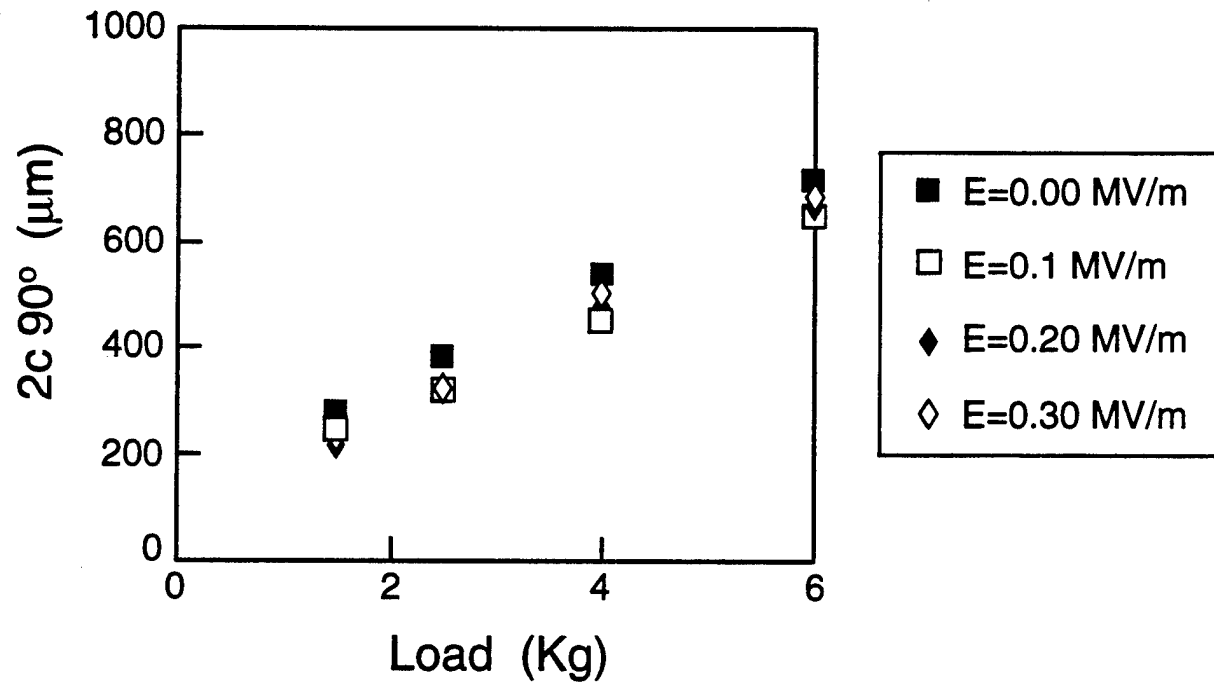
Figure 6. Indentations are performed in the presence of electric field on the 9.4/65/35 quadratic electrostrictive composition. The presence of electric field may slightly hinder crack growth, but the amount is not significant.
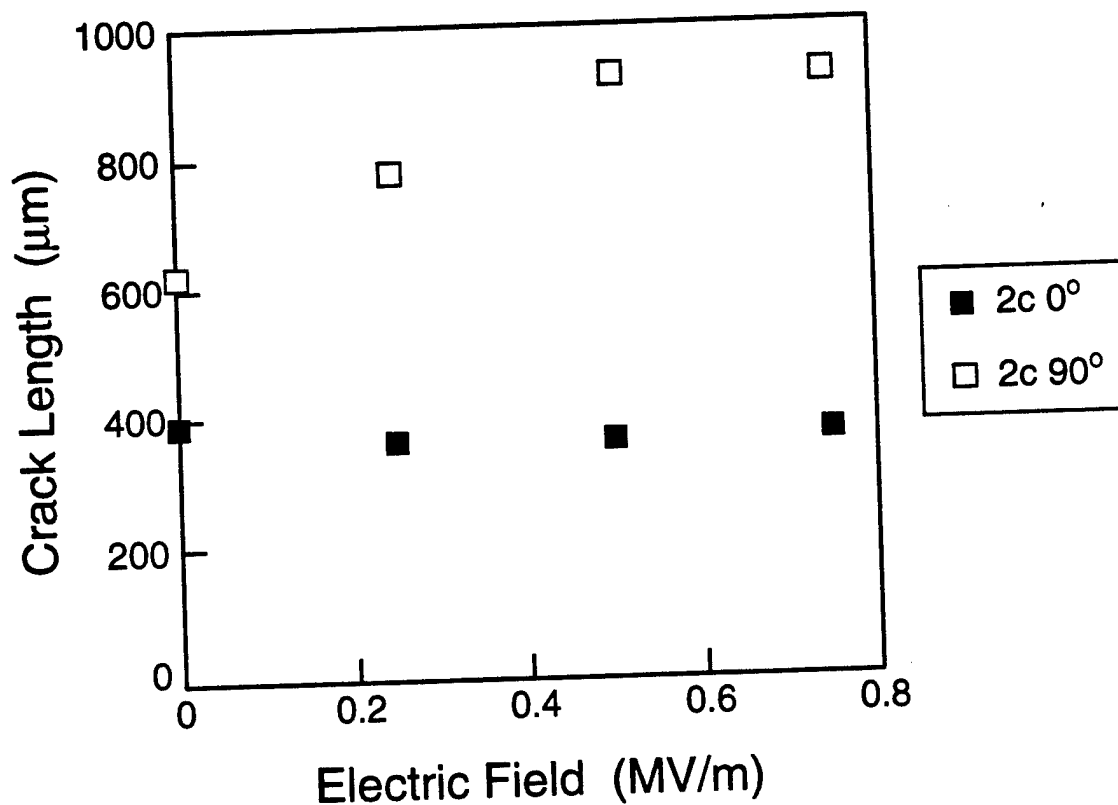
Figure 7. Indentations in the polarized 8/65/35 composition in the presence of electric field. As the electric field is increased, the cracks perpendicular to the polarization direction become longer. This effect saturates just above the coercive field.
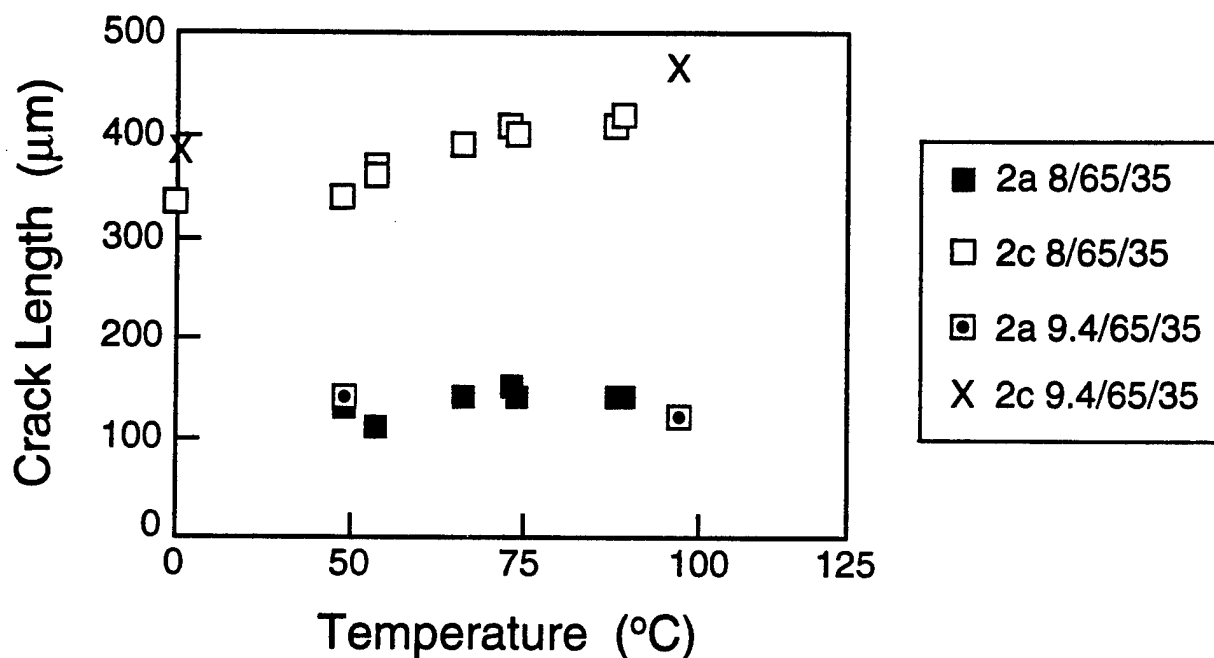
Figure 8. Crack length and indentation size produced by a 3 kg load are measured at various temperatures. The indentation size is independent of temperature. Crack growth increases with temperature. The 8/65/35 composition goes from ferroelectric to quadratic electrostrictive behavior over this temperature range. The 9.4/65/35 composition goes from quadratic electrostrictor to cubic paraelectric behavior over this temperature range. As the availability of twinning decreases, crack growth increases.

**J-Integral for Ferroelectric Compact Tension Specimens
with Electric Field**

Christopher S. Lynch

The G.W. Woodruff School of Mechanical Engineering
(Mechanics of Materials Group)
The Georgia Institute of Technology
Atlanta, Georgia 30332-0405

J-Integral for Ferroelectric Compact Tension Specimens with Electric Field

Christopher S. Lynch

Georgia Institute of Technology, School of Mechanical Engineering

Atlanta, Georgia 30332-0405

ABSTRACT

Experiments based on the compact tension geometry are applied to a relaxor composition of lead lanthanum zirconate titanate (PLZT). This composition is transparent, and displays electro-optical and piezo-optical coupling. A standard photo-stress arrangement (crossed polarizers and quarter wave plates) gives a direct view of electric field and stress concentrations. Electric field is observed to cause cracks to close. This is consistent with earlier predictions of a negative energy release rate.

keywords: ferroelectric, relaxor, compact tension, electric field, piezoelectric, PLZT

1. INTRODUCTION

Fracture toughness is a measure of a material's ability to resist crack growth. Many observations (most based on Vickers indentations[1,2,3]) indicate that stress and electric field interact with cracks in ferroelectric ceramics. In poled piezoelectrics, additional crack growth is observed perpendicular to the polarization direction. Recently there have been many efforts to extend the mathematical formalisms of fracture mechanics to ferroelectric ceramics. Asymptotic analysis has been done with assumed boundary conditions of an impermeable or conducting crack interior. This work presents direct observations of the effect of finite permittivity and finite dielectric strength within a notch or a crack.

2. EXPERIMENTS

2.1. Material Characteristics

PLZT (lead lanthanum zirconate titanate) is a relaxor ferroelectric. Specimens were produced from two compositions, 8/65/35 and 9.4/65/35 (at%La/PZ/PT). At room temperature 8/65/35 is ferroelectric and 9.4/65/35 is quadratic electrostrictive. These will be referred to as ferroelectric and relaxor compositions in the following discussion. The properties of both compositions are given in Table 1. They have a rhombohedral crystal structure and an average 5 μm grain size.

TABLE I. PROPERTIES OF PLZT[4]

Composition (%La/Zr/Ti)	8/65/325	9.5/65/35
d_{33} ($\times 10^{-12}$ C/N)	682	0
P^R (C/m^2)	0.30	0
Ec (MV/m)	3.6	0
Tc (°C)	110	25
25°C Phase	Ferro. Rh.	
ε_r	3350	5500
tan δ (%)	2.5	5.5
resistivity (Ω-cm)	10^{13}	10^{13}
k	0.648	0
S_{11} ($\times 10^{-12}$ m^2/N)	12.4	12.4
Q_{11} (m^4/C^2)	0.018	0.021
Q_{12} (m^4/C^2)	-0.008	-0.009

2.2 Test Technique

Specimens were cut to the dimensions shown (Fig. 1). They were then places in a servo-hydraulic test frame between crossed polarizers and quarter wave plates as shown (Fig. 2). A tensile load, a voltage, or both were applied. The voltage was applied to silver epoxy electrodes on the top and bottom of the specimen. The electrodes were insulated with epoxy to prevent arcing. Birefringence was observed at the front of the saw cut notch.
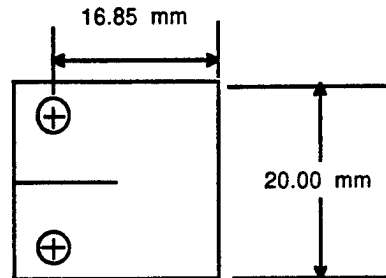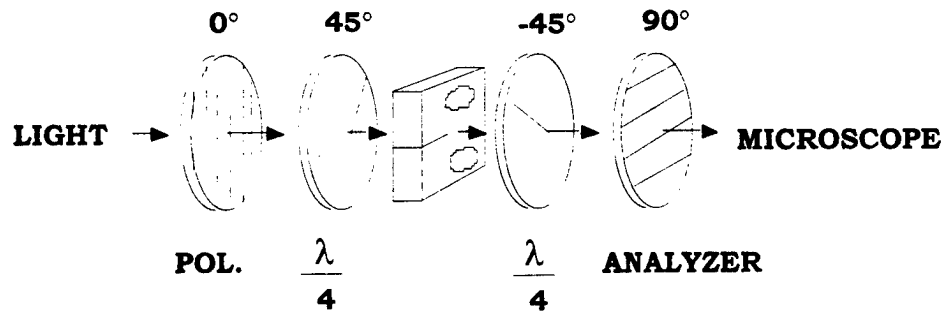
Figure 1. Compact Tension Specimen

Figure 2. Experimental arrangement for monitoring notch tip birefringence.

2.3 Results

2.3.1 Mechanical Load Only

When mechanical load is applied to the specimen, the pattern of birefringence is similar to that of a mode I stress concentration (Fig. 3). The micro-twinning that is responsible for the birefringence is shear induced. This gives rise to birefringence patterns of the same shape as those predicted for small scale yielding.

2.3.2 Electrical Load Only

When electric field is applied to the specimen, the pattern of birefringence is circular in shape. This is consistent with the asymptotic solution for electric field in a dielectric with an impermeable crack. The solution is the same in form as that of the Mode III stress field. This leads to circular patterns similar to the shape of a plastic zone ahead of a mode III crack.

Figure 3. Birefringence contours produced by tensile stress.

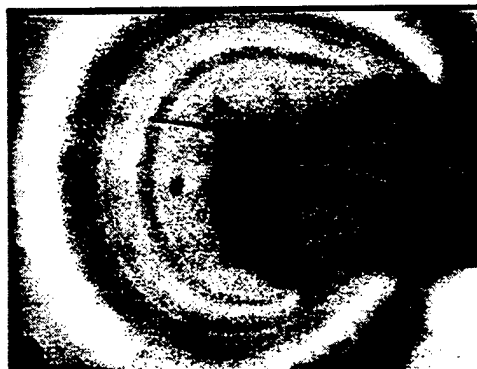Figure 4. Birefringence contours produced by electric field.

Figure 5. Electric field closes the crack, even when stress is present.

2.3.3 Electric field closes the crack

When the mechanical load was increased to 110 N, some stable crack growth occurred. The crack extended from the corner of the notch. The crack did not extend through the thickness of the specimen. The load was reduced to 60 N. At this point the crack was held open by the load. A 4000 V was then applied to the electrodes. As the voltage increased, the crack opening diminished. The voltage and stress were then reduced to zero and little or no residual birefringence were observed.

2.3.4 Evidence of Internal Arcing and Residual Charge

A voltage of 6000 V was applied next. When this voltage was reduced to zero, residual birefringence was observed (Fig. 6). This residual birefringence could be eliminated by application of 2000 V to the electrodes. The air within the notch or within the crack apparently ionized and distributed charge on the crack surfaces. This charge reduced the electric field concentration at the front of the notch.

Figure 6. Residual birefringence observed upon removal of a strong electric field.

3. DISCUSSION

3.1. Cracks in Permeable Dielectrics

Cracks with a low permittivity interior in a high permittivity material, that lie perpendicular to the electric field, concentrate the field at their tips[5-8]. This is clearly observed in the figures resented above. Polarizing PZT and BT by application of a strong electric field changes the toughness[7-13], with a decrease perpendicular to the polarization. A DC electric-field further changes the toughness[12,13]. Dielectric breakdown within notches or pores decreases electric field concentration by spreading a surface charge over the interior surface. This charge terminates the normal component of electric displacement.

3.1. J-Integral

The compact tension specimen is being developed as a J-integral test specimen. The energy release rate definition of J states that the external work done per unit crack advance is a measure of the toughness of the material. The external work can be directly measured by monitoring the load vs. displacement and the voltage vs. charge curves at several crack lengths.

ACKNOWLEDGEMENTS

REFERENCES

1. Anstis G.R., Chantikul, P., Lawn, B.R., Marshall, D.B., "A Critical Evaluation of Indentation Techniques for Measuring Fracture Toughness: I, Direct Measurements" *J. Am. Ceram. Soc*, **64** (9), 533-538, 1981

2. Braun L.M., S.J. Bennison, B.R. Lawn, "Objective Evaluation of Short Crack Toughness Curves Using Indentation Flaws: Case Study on Alumina-Based Ceramics", *J. Am. Ceram. Soc.,* 75[11] 3049-57 (1992)

3. Marshall D.B., B.R. Lawn, "An Indentation Technique for Measuring Stresses in Tempered Glass Surfaces", *J. Am. Ceram. Soc.* 60 [1,2] Jan-Feb (1977)

4. Lynch C.S., "The effect of uniaxial stress on the electro-mechanical response of 8/65/35 PLZT", Submitted to Acta. Met. (1995)

5. Suo Z., "Mechanics Concepts for Failure in Ferroelectric Ceramics", in *AD-Vol. 24/AMD-Vol. 123, Smart Structures and Materials, ASME Proceedings*, 1991

6. McMeeking, R.M., "Electrostrictive Stress near Crack-like Flaws," *J. Appl. Math. Phys.* **40**, 615-627 (1989)

7. Yang, W. and Z. Suo, "Cracking in Ceramic Actuators Coused by Electrostriction", *J. Mech. Phys. Solids*, 42[4], 649-63, (1994)

8. Suo, Z., "Models for Breakdown-Resistant Dielectric and Ferroelectric Ceramics," *J. Mech. Phys. Solids.* **41**, 1155-1176, 1993.

9. Pisarenko, G.G., V.M. Chushko, and S.P. Kovalev, "Anisotropy of Fracture Toughness of Piezoelectric Ceramics", *J. Am. Ceram. Soc.*, **68** [5] 259-65, 1985

10. Tobin A.G., Y.E. Pak, "Effect of electric field on fracture behavior of PZT ceramics", Proceedings SPIE Vol. 1916/79, March (1993)

11. Okazaki K., "Mechanical behavior of ferroelectric ceramics", Ceramic Bulletin, 63[9] (1984)

12. Sun C.T., S.B. Pak, "Determination of fracture toughness of piezoelectrics under the influence of electric field using Vicker's indentation", School of Aeronautics and Astronautics, Purdue University, unpublished work

13. Raynes A.S., G.S. White, S.W. Frieman, B.S. Rawal, "Electric field effects in a lead magnesium niobate ceramic", NIST (need reference)

14. Mehta K., A.V. Virkar, "Fracture Mechanisms in Ferroelectric-Ferroelastic Lead Zriconate Titanate (Zr:Ti=0.54:0.46) Ceramics", J. Am. Ceram. Soc. 73[3] 567-74 (1990)

15. Cao H.C., A.G. Evans, "Electric Field Induced Fatigue Crack Growth in Ferroelectric Ceramics", *J. Am. Ceram Soc* (in press 1995)

16. Lynch C.S., W. Yang, L. Collier, Z. Suo, R.M. McMeeking, "Electric FIeld Induced Cracking in Ferroelectric Ceramics", Accepted for Publication in Ferroelectrics, (1994)

Experimental Measurements of

Electro-Mechanical Constitutive Behavior of

Four Compositions of PZT

William A. Stoll and Christopher S. Lynch

The G.W.W. School of Mechanical Engineering

The Georgia Institute of Technology

Atlanta, Georgia 30332-0405

Abstract - Four compositions of commercially available PZT are characterized under combined stress and electric field loading. The loading consists of a series of increasing compressive stress increments alternating with a series of bipolar electric field cycles. The softest composition has the lowest Young's modulus and shows hysteresis in the electric field cycle that increases as the compressive stress is increased. A distinct yield stress associated with the onset of deformation twinning (depolarization) is evident at around 25 Mpa. After loading to 180 Mpa and unloading, there is a large residual strain. The hardest composition has a higher Young's modulus, shows little or no hysteresis in the electric field cycle until the compressive stress has been applied, has a distinct yield point at around 75 Mpa associated with the onset of deformation twinning, and after loading to 180 Mpa and unloading the non-linear strain is recovered. There is no residual strain. The two compositions that lie between the extremes display intermediate behavior.

1. INTRODUCTION

The selection of an active material for the design of an actuator system is often based on the d_{33} linear piezoelectric coefficient and the loss tangent. These coefficients are measured at small field and are not adequate for predicting the behavior under large electric field or stress. This work presents the results of an experimental survey of several compositions of PZT under high stress and electric field loading.

The recent interest in developing PZT as an actuator material for large force and displacement applications has pushed the use of the materials beyond the regime where there is design data. Operating the material at high stress and electric field levels results in non-linear and irreversible behavior. This is associated with deformation twinning (depolarization by 90° domain wall motion in the tetragonal case) when critical stress and electric field levels are exceeded. A combination of stress and electric field acting simultaneously can reduce the levels that cause depolarization.

The properties that are most familiar to users are those measured at small stress and electric field, usually using an acoustic resonance technique [1]. The linear properties [2] and the loss tangent are published by most of the suppliers of PZT. Reported stress/strain curves [3] and detailed measurements of the stress/strain/electric-field behavior of 8/65/35 PLZT [4] led to this survey of several compositions of soft and hard commercially available materials. Creep and stress relaxation [5] (associated with aging) are not addressed in this work.

There has been relatively little modeling of constitutive behavior from the mechanics perspective. An elementary micromechanics model [6] was developed for tetragonal materials. This model simulates the electric-displacement/electric-field, strain/electric-field, and stress-strain behavior with some success. An extension of the model is needed to include a back stress and back electric field that induce strain and polarization recovery, the ability to simulate the rhombohedral geometry, and the interaction effects between the grains of the ceramic. Phenomenological models of multiaxial deformation twinning induced by stress and electric field are still needed for finite element calculations of material response. This will facilitate computational studies of non-uniform material loading such as occurs in the fracture process and in complex transducer designs.

These models have not been developed largely due to a lack of data. Experimental techniques for this type of measurement have only recently been developed. This work presents a survey of four commercially available compositions under combined stress and electric field loading. The loading is isothermal (room temperature) and quasi-static. The materials range from soft to hard. These are terms used to describe the effects of dopants [7].

2. MATERIALS

The materials were obtained in a prepoled state from a commercial source [8]. The manufacturer's names for the various compositions are listed in each figure. A loading fixture (Fig. 1) was developed to simultaneously apply compressive stress and electric field.
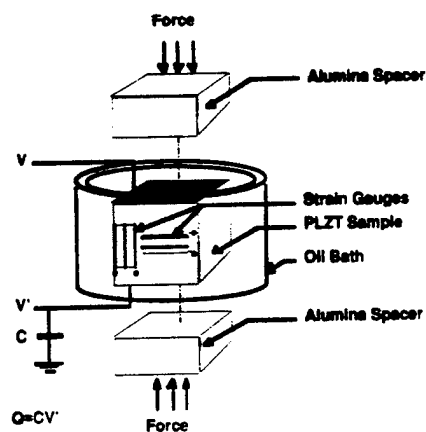

Figure 1. Combined compressive stress and electric field loading fixture.

3. EXPERIMENTAL RESULTS

The data presented below (Figs. 2-5) describe the behavior of PZT ranging from soft to hard under combined stress and electric field loading. Starting at zero stress and strain the electric field is positively cycled to approximately -0.7 MV/m and then back to zero. Next, it is negatively cycled to -.07 MV/m then back to zero. The stress is then increased at zero electric field. Holding the stress constant, the electric field is cycled again. This loading is repeated until the sample is unloaded at zero electric field. Several features are of note. The soft composition has depoled after the stress is removed. This results in a residual strain of about 6000 microstrain. (See [4] for a detailed discussion of depolarization and loss of remanent strain.) The hard material depoles, but the internal field causes it to spontaneously repole when the stress is removed. There is no residual strain. Also, the hysteresis seen in the zero stress electric field cycle of the soft material is associated with the large loss tangent and low Q. This does not occur in the hard material.
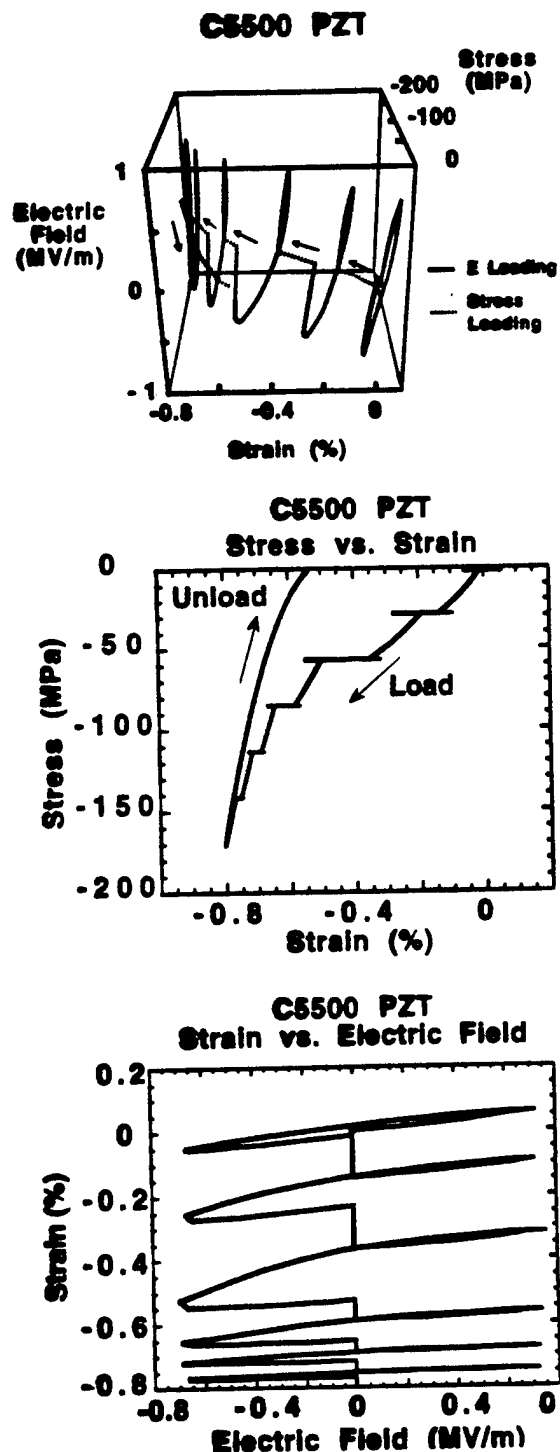

Figure 2. Softest composition of PZT tested. Full stress/strain/electric-field cycle (top). Stress/strain cycle (middle). Strain/electric-field (bottom). Note the low elastic modulus and the large d_{33}. These are associated with domain wall motion and hysteresis. This material is easily depoled.

2

C5400 PZT

C5804 PZT

C5400 PZT
Stress vs. Strain

C5804 PZT
Stress vs. Strain

C5400 PZT
Strain vs. Electric Field

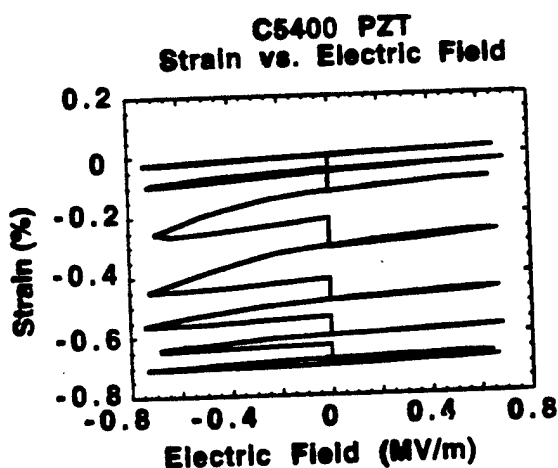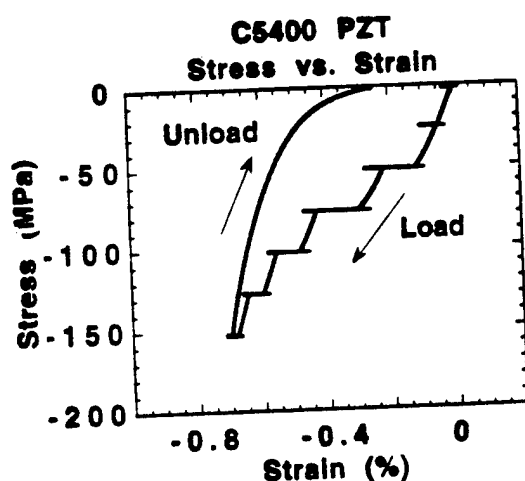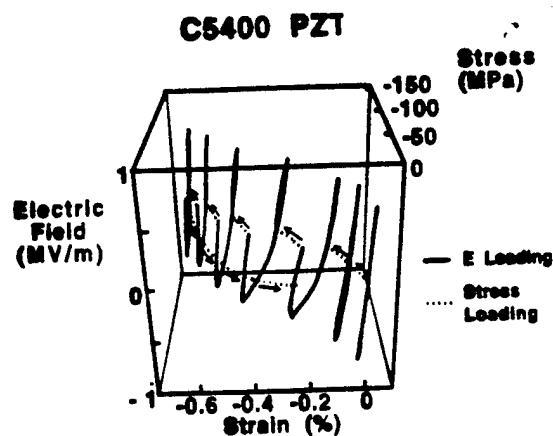**C5804 PZT**
Strain vs. Electric Field

Figure 3. Intermediate/soft composition of PZT. Full stress/strain/electric-field cycle (top). Stress/strain cycle (middle). Strain/electric-field (bottom). Note the increased elastic modulus and some strain recovery after the stress is removed.
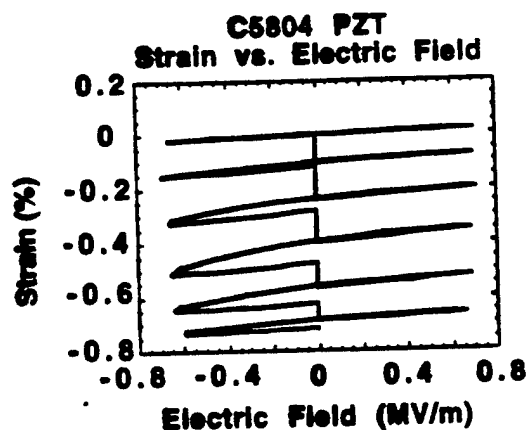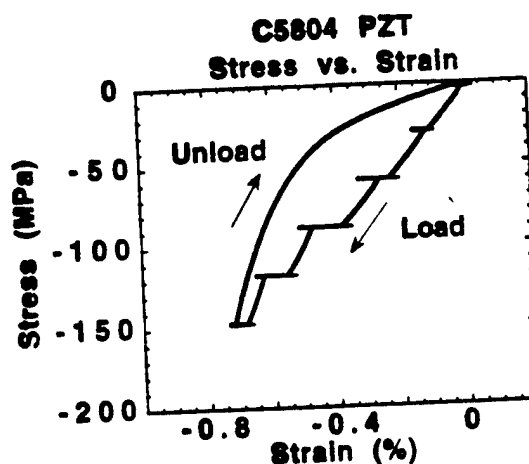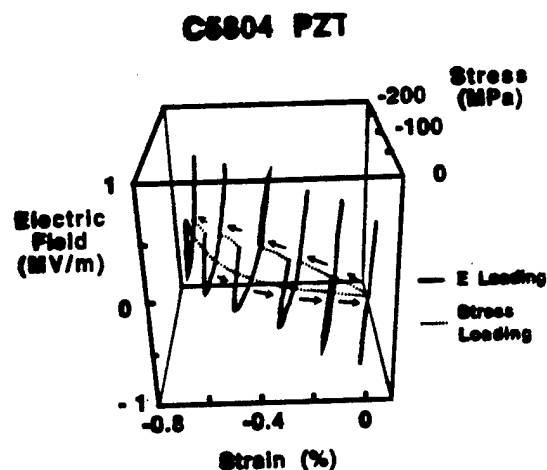
Figure 4. Intermediate/hard composition of PZT. Full stress/strain/electric-field cycle (top). Stress/strain cycle (middle). Strain/electric-field (bottom). Note the further increased elastic modulus and full strain recovery after the stress is removed.

3

C5800 PZT

C5800 PZT
Stress vs. Strain
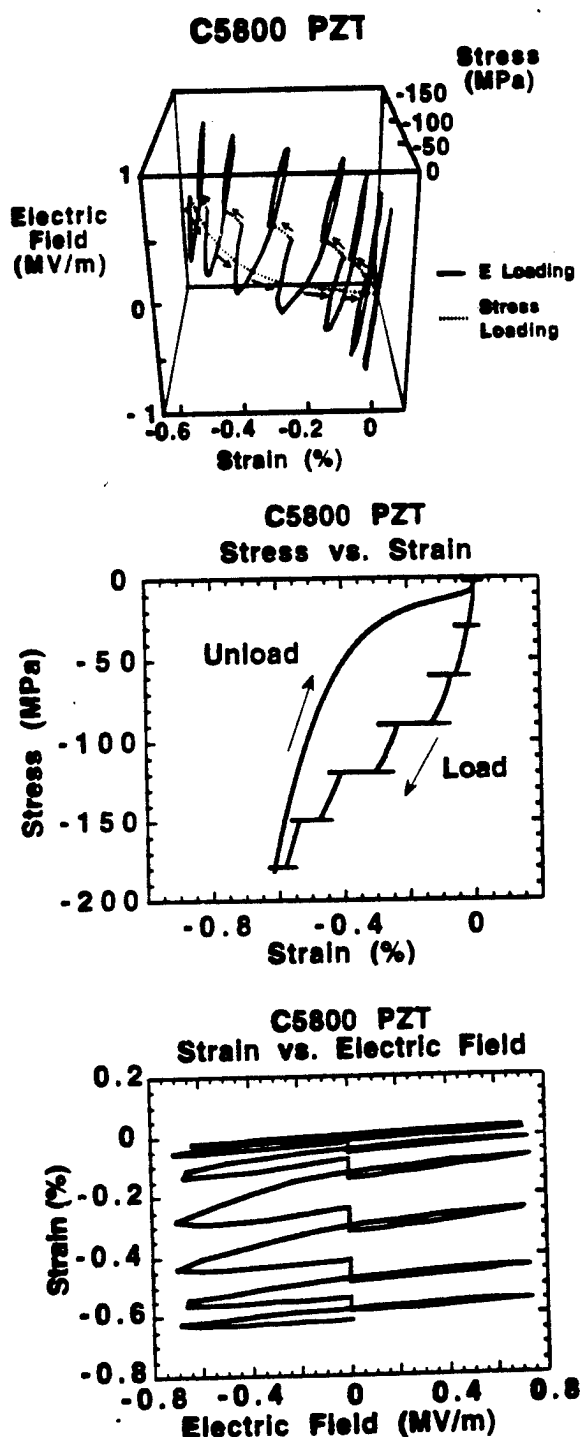

C5800 PZT
Strain vs. Electric Field

Figure 5. Hardest composition of PZT tested. Full stress/strain/electric-field cycle (top). Stress/strain cycle (middle). Strain/electric-field (bottom). Note the high elastic modulus and full strain recovery even before the stress is fully unloaded.

4. CONCLUDING REMARKS

The softest composition has the lowest elastic modulus (slope of the stress/strain curve) and highest d_{33} coefficient (slope of the strain/electric-field curve). In actuator applications, the high d_{33} coefficient does not make up for the lower blocking load. The hard compositions do not begin to depolarize until the stress level has exceeded 50 to 75 MPa or more. The soft compositions depole at much lower stress level. This further limits their application as actuators. The hard compositions have far less hysteresis in the strain/electric-field response. This makes them better candidates for micro-positioning applications. The strain recovery upon unload of the stress in the hard compositions gives a more robust design for actuator applications. An occasional stress overload does not permanently depole the ceramic.

All of these tests were run in about a one hour time frame. The hard materials will quite likely permanently depole if subjected to a compressive stress for a long duration. The tests were also conducted at room temperature. At elevated temperature, permanent depolarization of the hard material is expected to occur under compressive stress loads. Further work is needed in this area before reliable device design can be accomplished.

5. ACKNOWLEDGMENTS

6. REFERENCES

[1] Cady, W.G. Piezoelectricity, Dover, N.Y, 1964
[2] Lines and Glass, "Principles and Applications of Ferroelectrics and Related Materials", Oxford 1977
[3] Cao H.C., A.G. Evans, "Nonlinear Deformation of Ferroelectric Ceramics", J. Am. Ceram. Soc., 76[4] 890-96, (1993)
[4] Lynch C.S., "The effect of uniaxial stress on the electro-mechanical response of 8/65/35 PLZT", Submitted to Acta. Met. (1995)
[5] Esaklul K.A., W.W Gerberich, B.G. Koepke, "Stress relaxation in PZT", J. Am. Ceram. Soc. 63[1,2], 25-30, (1980)
[6] Hwang S.C., C.S. Lynch, and R.M. McMeeking, "Ferroelectric/Ferroelastic Interactions and a Polarization Switching Model", Accepted for publication in Acta Met. June 1994
[7] Jaffe B., W.R. Cook, and H. Jaffe, "Piezoelectric Ceramics". p 162, Academic Press London and New York, 1971.
[8] Channel Industries, Goleta, California